Phosphodiesterase 4D promotes angiotensin II-induced hypertension in mice via smooth muscle cell contraction

Tianfei Fan
Institute of Basic Medical Science, Chinese Academy of Medical Sciences & Peking Union Medical College

Yangfeng Hou
Institute of Basic Medical Science, Chinese Academy of Medical Sciences & Peking Union Medical College

Weipeng Ge
Institute of Basic Medical Science, Chinese Academy of Medical Sciences & Peking Union Medical College

Tianhui Fan
Institute of Basic Medical Science, Chinese Academy of Medical Sciences & Peking Union Medical College

Wenjun Guo
Institute of Basic Medical Science, Chinese Academy of Medical Sciences & Peking Union Medical College

Xiaomin Song
Institute of Basic Medical Science, Chinese Academy of Medical Sciences & Peking Union Medical College

Ran Gao
Institute of Basic Medical Science, Chinese Academy of Medical Sciences & Peking Union Medical College

Jing Wang (✉ wangjing@ibms.pumc.edu.cn)
Institute of Basic Medical Science, Chinese Academy of Medical Sciences & Peking Union Medical College https://orcid.org/0000-0003-2410-5408

Article

Keywords: PDE4D, hypertension, PKA, AMPK, vasocontraction

Posted Date: March 29th, 2021

DOI: https://doi.org/10.21203/rs.3.rs-344201/v1

Version of Record: A version of this preprint was published at Communications Biology on January 20th, 2022. See the published version at https://doi.org/10.1038/s42003-022-03029-0.

Abstract

Hypertension is a common chronic disease, which leads to cardiovascular and cerebrovascular diseases, and its prevalence is increasing. Cyclic adenosine monophosphate (cAMP)-protein kinase A (PKA) pathway participates in multiple cardiovascular diseases. Phosphodiesterase (PDE) 4 has been shown to regulate PKA activity via cAMP specific hydrolysis. However, whether PDE4-cAMP-PKA pathway influences hypertension remains unknown. Herein, we reveal that PDE4D (one of PDE4 isoforms) expression is upregulated in angiotensin II (Ang II)-induced hypertensive mice aortas. Furthermore, knockout of *Pde4d* in mouse smooth muscle cells (SMCs) attenuate Ang II-induced high BP, arterial wall media thickening, vascular fibrosis and vasocontraction. Upon further investigation, we find that *Pde4d* deficiency activate PKA-AMP-activated protein kinase signaling pathway to inhibit myosin phosphatase targeting subunit 1-myosin light chain phosphorylation, relieving Ang II-induced SMC contraction *in vitro* and *in vivo*. These results indicate that PDE4D may be a potential target for hypertension therapy.

Introduction

Hypertension defined as an arterial systolic and diastolic blood pressure (BP) > 140/90 mmHg by European Society of Cardiology/European Society of Hypertension[1]. While generally asymptomatic, hypertension is a severe risk factor for cardiovascular diseases, strokes, and kidney diseases[2]. Hypertension occurs through multiple pathogeneses, including sympathetic activation[3], the renin-angiotensin-aldosterone system disorder[4], inflammation[5], and endothelial cell (EC) and smooth muscle cell (SMC) dysfunction[6,7]. Presently, most hypertension medicines have adverse effects—headaches, oedema, and hyperkalaemia—which limit their application[8]. It is therefore imperative to develop potential hypertension treatments.

Phosphodiesterase (PDE), consisting of 11 subfamilies (PDE1-PDE11), is the hydrolase of cyclic adenosine monophosphate (cAMP) and cyclic guanosine monophosphate (cGMP). Moreover, PDE4, consisting of 4 isoforms (PDE4A-D), are cAMP specific hydrolases[9]. PDE4 participates in a variety pathophysiological processes[10], promoting SMCs' phenotypic switch and neointima formation in atherosclerosis[11], as well as aggravating pulmonary arterial hypertension through the regulation of vascular tone and inflammatory factors[12].

As a specific target for PDE4 hydrolysis, cAMP is related to cardiovascular diseases: cardiac fibrosis, abdominal aortic aneurysm, atherosclerosis, and pulmonary arterial hypertension[13–16]. In addition, the association between cAMP and these diseases was mainly established through its effector protein kinase A (PKA)[15]. However, the roles of PKA and its regulator PDE in hypertension remain unknown. Furthermore, PKA has been shown to activate AMP-activated protein kinase (AMPK)[17]. AMPK inhibitor aggravated SMCs contraction and hypertension by activating MYPT1-MLC signaling pathway[18]. As known, one of the pathological processes of hypertension is vasoconstriction, and MYPT1-MLC is a classical cell

contraction signaling pathway[19]. Therefore, it is hypothesized that PDE4 may affect SMCs contraction by PKA-AMPK-MYPT1-MLC pathway and thus affect hypertension.

In this study, we found that PDE4D expression was upregulated in aortic tissues of hypertensive mice. Furthermore, PDE4D was expressed in SMCs instead of ECs, contributing to hypertension development. In addition, we demonstrated that PDE4D promoted SMCs contraction and vasocontraction via PKA-AMPK-MYPT1-MLC signaling pathway.

Results

Phosphodiesterase 4D (PDE4D) expression is upregulated in angiotensin (Ang) II-induced hypertensive mice

We first established a hypertensive model in wild-type mice (Supplementary Fig. 1a, b). To initially investigate PDE4 expression after hypertension, we evaluated mRNA levels of each PDE4 isoform (*Pde4a-d*) in control and hypertensive mice thoracic aortas. The results revealed a significant increase in *Pde4d* mRNA level between the two groups (Fig. 1a). Consistently, PDE4D protein expression was increased in hypertensive mice according to western blot and immunohistochemical staining (Fig. 1b-e). Together, these findings indicate that PDE4D expression is significantly elevated in Ang II-induced hypertensive mice aortas.

PDE4D in smooth muscle cells (SMCs) contributes to Ang II-induced mice hypertension

Among vascular intrinsic cell types, endothelial cell (EC) and smooth muscle cell (SMC) are known to play crucial roles in hypertension formation[6,7]. To explore whether PDE4D, via SMCs or ECs, plays an analogous role in hypertension, we generated *Pde4d* SMC-specific knockout mice ($PDE4D^{SMC-/-}$) and *Pde4d* EC-specific knockout mice ($PDE4D^{EC-/-}$) mice via Cre-LoxP recombinase system, and confirmed the mice genotypes by agarose gel electrophoresis genotyping and western blot (Supplementary Fig. 2a-e).

We then induced hypertension in 2 knockout mice groups. Using the tail-cuff method, we measured BP on the first day and every other day during infusion; after 2 weeks we harvested the aorta tissues (Fig. 2a). Notably, EC *Pde4d* deficiency ($PDE4D^{flox/flox}$ + Ang II group vs. $PDE4D^{EC-/-}$ + Ang II group) did not affect the occurrence or development of the Ang II-induced systolic blood pressure (SBP; 139.3 ± 2.47mmHg vs. 139.45 ± 2.56 mmHg) or diastolic blood pressure (DBP; 116.85 ± 2.47 mmHg vs. 117.1 ± 3.73 mmHg; Fig. 2b, c). However, SMC *Pde4d* deficiency ($PDE4D^{flox/flox}$ + Ang II group vs. $PDE4D^{SMC-/-}$ + Ang II group) inhibited the Ang II-induced increase of both SBP (149.98 ± 1.78 mmHg vs. 127.43 ± 2.97 mmHg) and DBP (122.48 ± 1.35 mmHg vs. 99.4 ± 2.55 mmHg; Fig. 2d, e). Hematoxylin and eosin (H&E) staining revealed that Ang II significantly induced vessel wall media thickening, which was significantly reduced in $PDE4D^{SMC-/-}$ Ang-II infused mice (Fig. 2f, g). In addition, masson-trichrome staining demonstrated that SMC *Pde4d* deficiency significantly reversed Ang II-induced vascular fibrosis (Fig. 2h, i). These results indicate that PDE4D in SMCs, but not in ECs, contribute to Ang II-induced mice hypertension.

SMC Pde4d deficiency reduces vasocontraction

To further explore how PDE4D in SMCs influences hypertension, we examined direct vascular function in the knockout mice. Specifically, the *ex vivo* vascular function of intact mesenteric arteries from $PDE4D^{flox/flox}$ and $PDE4D^{SMC-/-}$ mice with or without Ang II treatment. Using phenylephrine (PE) and Ang II to induce mesenteric arteries contraction, we found that the vasocontraction was markedly suppressed in $PDE4D^{SMC-/-}$ mice compared with $PDE4D^{flox/flox}$ mice ($PDE4D^{flox/flox}$ + Ang II group vs. $PDE4D^{SMC-/-}$ + Ang II group; 10^{-5} M PE: 175.53 % ± 5.52 % vs. 130.42 % ± 10.79 %; 10^{-7} M Ang II: 214.38 % ± 25.3 % vs. 132.08 % ± 12.6 %) (Fig. 3a, b). These findings further support that SMC *Pde4d* deficiency relieves vasocontraction.

PDE4D promotes SMCs contraction via the PKA-AMPK-MYPT1-MLC signaling pathway in vitro

To determine PDE4D's role in regulating SMC contraction, we evaluated its impact on rat aorta smooth muscle cells (RASMCs) *in vitro*. First, we verified that PDE4D protein expression was elevated by 5.37 folds in RASMCs after Ang II (100 nM, 24 h) stimulation (Fig. 4a, b). Then, we introduced PDE4D small interfering RNA (siRNA) to validate whether Ang II-induces SMCs contraction via PDE4D. After PDE4D siRNA administration, PDE4D expression was significantly reduced in RASMCs' mRNA and protein levels (Supplementary Fig. 3a-c). We next performed a collagen gel cell contraction assay to explore RASMCs contraction, which revealed that while Ang II promoted RASMC contraction, the addition of PDE4D siRNA inhibited it (si-control + Ang II vs. si-PDE4D + Ang II: 72.68 % ± 2.11 % vs. 58.65 % ± 1.76%) (Fig. 4c, d).

PDE4 family specifically hydrolyzes cAMP to inhibit protein kinase A (PKA) activity[20–22]. PKA phosphorylates AMPKα at Thr-172 through LKB1 signaling, ultimately leading to AMPK activation [17,23–27]. As such, we investigated whether PDE4D inhibited PKA and AMPK activity in RASMCs. Consistently, we found that Ang II stimulation reduced PKA activity in RASMCs, and that PDE4D siRNA reversed this effect (Fig. 4e). Moreover, we observed that PDE4D siRNA increased Ang II-reduced AMPK phosphorylation (Fig. 4f, g).

Additionally, AMPK activation inhibits phosphorylation of myosin phosphatase targeting subunit 1 (MYPT1) and myosin light chain (MLC), consequently attenuating SMCs contraction[18]. Therefore, we hypothesized that PDE4D may further increase MYPT1 and MLC phosphorylation by suppressing AMPK activation, promoting Ang II-induced SMCs contraction. Indeed, Ang II increased MYPT1 and MLC phosphorylation, whereas PDE4D siRNA suppressed MYPT1 and MLC phosphorylation (Fig. 4f, h, i). These results suggest that PDE4D promotes SMCs contraction via inhibition of PKA activity and AMPK phosphorylation, and conversely promotes MYPT1 and MLC phosphorylation.

PDE4D promotes vasocontraction through the PKA-AMPK-MYPT1-MLC signaling pathway in Ang II-induced mice hypertension

To further validate the mechanism identified *in vitro* above, we detected PKA activity and AMPK, MYPT1, and MLC phosphorylation in mice aorta tissues. Consistently, Ang II infusion reduced PKA activity in mice

aortas, and this reduction was reversed in PDE4D$^{SMC-/-}$ Ang II mice (Fig. 5a). Western blot also exhibited that Ang II infusion reduced AMPK phosphorylation in the aorta, an effect which was recovered in PDE4D$^{SMC-/-}$ mice (Fig. 5b, c). Ang II infusion also increased MYPT1 and MLC phosphorylation, and again PDE4D$^{SMC-/-}$ mice exhibited reduced Ang II-induced MYPT1 and MLC phosphorylation (Fig. 5b, d, e). These results suggest that PDE4D promotes vasocontraction, and thus contributes to Ang II-induced hypertension in mice, through the PKA-AMPK-MYPT1-MLC signaling pathway (Fig. 6).

Discussion

In this study, we observed upregulated PDE4D expression in hypertensive mice aortas, and exhibited that PDE4D contributes to hypertension. Furthermore, via EC- and SMC-specific *Pde4d* knockout hypertensive mice., these models revealed a causal association between SMC *Pde4d* and vasocontraction in hypertension. To further elucidate this association, we investigated a potential mechanism for PDE4D involvement in SMC contraction and hypertension development, and identified the PKA-AMPK-MYPT1-MLC signaling pathway to be a likely candidate. Our findings suggest that PDE4D might represent a potential therapeutic hypertension target.

Hypertension is well known to be a complex syndrome involving multiple organs, tissues, and cells[28,29]. Among the cell types associated with hypertension, PDE4D is also expressed in fibroblasts[30,31]. Adventitial fibroblasts, another major component of blood vessels, are the primary cause of collagen deposition and aortic stiffening in hypertension[32]. In this study, we observed vascular collagen deposition in Ang II infusion mice. Accordingly, it should not be discounted that PDE4D could further contribute to the development of hypertension by interfering with collagen production in fibroblasts, a possibility warranting future investigation.

Hypertension is commonly associated with inflammation[33,34], and the cell types involved in inflammation (T lymphocytes[35], B lymphocytes[36,37], dendritic cells, monocytes, and macrophages[38]) are all known to promote hypertension. PDE4D has been shown to interact with cytokines, regulate the function of inflammatory cells, and aggravate the inflammatory response[39–41]. While PDE4D's role in the inflammation response is outside the scope of this study, this study's findings, along with the body of literature evidence, suggest that PDE4D could also contribute to hypertension via inflammation regulation. Although, further study would be needed to validate this supposition.

While collagen deposition and inflammation may be potential additional mechanisms, we demonstrated a link between PDE4D and the PKA-AMPK signaling pathway. cAMP is known to be involved in signal transduction through PKA regulation[42]. Recently, researchers have found that PKA phosphorylates AMPKα at Thr-172 through the widely expressed tumor suppressor liver kinase B1 (LKB1), ultimately activating AMPK[17,27]. AMPK activity has been linked to numerous cardiovascular diseases, including hypertension, atherosclerosis, and heart failure[18,43–45]. Crucially, AMPK activation lowers BP and suppresses SMC contractility by inhibiting the MYPT1-MLC signaling pathway[18]. Consistent with

previous reports, our results exhibited that PDE4D upregulated MYPT1 and MLC phosphorylation by inhibiting the PKA-AMPK signaling pathway, inducing SMCs contraction and thereby, hypertension.

In conclusion, our study provides that PDE4D in SMCs aggravates Ang II-induced hypertension. We identified the mechanism by which PDE4D affects SMCs contraction via *in vitro* and *in vivo* experimental models and verified those results through several molecular biology approaches. This study elucidates PDE4D as a potential target for the treatment of hypertension and, potentially, other cardiovascular diseases.

Materials And Methods

Animal models

Pde4d -floxed (flanked by LoxP) mice ($PDE4D^{flox/flox}$), Tagln-Cre mice, and Tek-Cre mice were generated and obtained by Shanghai Model Organisms Center, Inc. (Shanghai, China). To generate smooth muscle cell (SMC)-specific knockout mice ($PDE4D^{SMC-/-}$) or endothelial cell (EC)-specific knockout mice ($PDE4D^{EC-/-}$), $PDE4D^{flox/flox}$ was crossed with Tagln-Cre mice or Tek-Cre mice (Shanghai Model Organisms Center). Genotyping was performed by polymerase chain reaction (PCR) using primers (Supplementary Table 1). $PDE4D^{flox/flox}$, $PDE4D^{SMC-/-}$, and $PDE4D^{EC-/-}$ littermates were used in this research. Wild-type (WT) mice (C57BL/6, N11) were obtained from The Jackson Laboratory (Bar Harbor, ME). All mice were housed in temperature-controlled rooms under a 12-hour light-dark cycle with water and food *ad libitum*.

To induce hypertension in $PDE4D^{flox/flox}$, $PDE4D^{SMC-/-}$, $PDE4D^{EC-/-}$, and WT mice, 8-week old male mice were infused with angiotensin II (Ang II, 490 ng kg^{-1} min^{-1}; Sigma, Cat#: A9525-50MG) or saline and subcutaneously implanted with osmotic pumps (Alzet MODEL 2004; DURECT, Cupertino, CA) for 14 days[46]. Mice groups: WT mice were divided into 2 groups, WT mice infused with saline (n = 4) or Ang II (n = 8); $PDE4D^{EC-/-}$ mice were divided into 4 groups, $PDE4D^{flox/flox}$ mice infused with saline (n = 5) or Ang II (n = 8), and $PDE4D^{EC-/-}$ mice infused with saline (n = 5) or Ang II (n = 8); $PDE4D^{SMC-/-}$ mice were divided into 4 groups, $PDE4D^{flox/flox}$ mice infused with saline (n = 5) or Ang II (n = 10), and $PDE4D^{SMC-/-}$ mice infused with saline (n = 5) or Ang II (n = 8). All animal protocols were reviewed and approved by the Ethics Committee of Peking Union Medical College.

BP measurement by tail-cuff plethysmography

SBP and diastolic DBP in mice were measured using the CODA non-invasive BP system (Kent Scientific Co., Torrington, CT, USA) according to the manufacturer's instructions[47]. Each mouse was gently placed in a sizeable holder and allowed to acclimate for 5 minutes. The tail was then threaded through the occlusion cuff and the sensor cuff, which was then attached to the controller. For each measurement, 5 values of SBP and diastolic DBP were recorded for each mouse and their mean values used as the final result.

Measurement of mesenteric artery tension

Mice were euthanized under pentobarbital sodium (50 mg kg^{-1}, intraperitoneal). The mesenteric vascular bed was quickly removed, and immersed in Krebs bicarbonate buffer (119 mM NaCl, 25 mM $NaHCO_3$, 4.7 mM KCl, 1 mM $MgCl_2$, 1.2 mM KH_2PO_4, 2.5 mM $CaCl_2$, and 11 mM D-glucose) and gassed with a mixture of 95% O_2 and 5% CO_2[48]. Second-order branches of the mesenteric artery (approximately 2 mm long segments) were suspended with two tungsten wires in the organ chamber containing 5 mL of Krebs buffer solution. The vasocontraction was examined by phenylephrine (PE) or Ang II. Changes in isometric force were recorded with a Multi Myograph System (610 M, Danish Myo Technology A/S, Aarhus N, Denmark) according to the manufacturer's instruction. The relative contraction was quantified as the ratio of post stimulation tension to baseline tension.

Histological and immunohistochemical analysis

Mouse aorta segments were cut at the thoracic aorta, embedded vertically with OCT compound (SAKURA, Cat#:4538), and then stored at − 80°C. Ten to fifteen serial frozen sections containing the entire vascular lumen were sectioned using a freezing microtome (Leica CM1860), and then fixed with 4% paraformaldehyde. Frozen sections (6 μm) were stained by immunohistochemical staining of PDE4D (1:100, Abcam, Cat#: ab14613) by the 3-amino-9-ethylcarbazole (AEC) staining method, hematoxylin and eosin (H&E; Solarbio, Cat#: G1120), and masson-trichrome staining (Servicebio, Cat#: G1006). Images were photographed using a Leica optical microscope (Leica Microsystems, Germany) and the integrated optical density values of positive staining analyzed using Image-Pro Plus software (Media Cybernetics, USA). For statistical analysis, 5 images per mouse of each group were randomly selected. The content of PDE4D was quantified as the ratio of positively stained area to the total cross-sectional area of the aortic wall.

Real-time polymerase chain reaction (RT-PCR)

Total RNA was extracted from mouse aortic tissues or rat aorta smooth muscle cells (RASMCs) using TRIzol reagent (Invitrogen, Carlsbad, CA, Cat#: 15596018) according to the manufacturer's protocol. Equal quantities of RNA (1000 ng) were reverse transcribed into cDNA (TianGen, KR116-02), and quantitative RT-PCR was performed in a single-colour RT-PCR detection system (Bio-Rad, Hercules, CA, USA). The mRNA levels of *Pde4a*, *Pde4b*, *Pde4c*, and *Pde4d* were normalized to the level of the housekeeping gene glyceraldehyde-3-phosphate dehydrogenase (*Gapdh*). *Pde4a*, *Pde4b*, *Pde4c*, and *Pde4d* mRNA expression fold changes compared to the control group, or single control mouse, were calculated using the $2^{-\Delta\Delta Ct}$ method. The RT-PCR primers are shown in Supplementary Table 1.

Western blot analysis

Protein was extracted from the aortic tissues or RASMCs in a lysis buffer. Equal quantities of protein extract (30 μg per lane) were separated by 8%, 10% or 12% SDS–PAGE and transferred to a polyvinylidene fluoride membrane. The target protein was probed with numerous antibodies: PDE4D (1:1000, Abcam, Cat#: ab171750), AMP-activated protein kinase (AMPK; 1:1000, Cell Signaling Technology, Cat#: 2532S), Phospho-AMPK (1:1000, Cell Signaling Technology, Cat#: 2535S), myosin phosphatase targeting subunit 1 (MYPT1; 1:1000, Cell Signaling Technology, Cat#: 2634S), Phospho-MYPT1 (1:500, Cell Signaling

Technology, Cat#: 5163S), myosin light chain (MLC; 1:1000, Cell Signaling Technology, Cat#: 8505S), and Phospho-MLC (1:1000, Cell Signaling Technology, Cat#: 3675S), respectively. Immunoblotting of the housekeeping protein GAPDH (1:5000, Proteintech, Cat#: 60004-1-Ig) was performed to ensure equal protein loading. Immunoreactive bands were visualized with SuperSignal™ West Pico PLUS Chemiluminescent Substrate (Pierce, Cat#: 34577). The protein expression was measured by analyzing the relative protein band intensity with Image-Pro Plus 6.0 software.

Protein Kinase A (PKA) kinase activity assay

Protein Kinase A (PKA) kinase activity in aortic tissues or RASMCs was detected via a PKA kinase activity assay kit (Abcam, Cat#: ab139435) according to the manufacturer's instructions. Absorbance was measured at optical density (OD) = 450 nm via a multi-mode microplate reader (BioTek Synergy™ HTX, BioTek Instrument, Inc., Winooski, USA). The relative activity of PKA was quantified as the ratio of the active PKA content to the sample total protein content.

Cell culture and small-interfering RNA (siRNA) transfection

RASMCs were purchased from American Type Culture Collection (Manassas, VA, USA) and cultured in SMC medium (ScienCell, Cat#: 1101), containing 5% fetal bovine serum (FBS), 100 U/mL penicillin, and 100 g/mL streptomycin. RASMCs within passage 5 to 12 were used for all experiments. RASMCs were stimulated with 100 nM Ang II (Sigma, Cat#: A9525-50MG) for 24 hrs before harvest. To knockdown *Pde4d*, PDE4D siRNA (Ribobio, siB180730051733) and control siRNA (Ribobio, siN0000001-1-5) were purchased from Ribobio (Guangzhou RiboBio Co., Ltd., Guangzhou, China). RASMCs were transfected with 200 nM PDE4D siRNA in 5 μL of Oligofectamine (Invitrogen, Carlsbad, CA, USA, Cat#: 12252011) for 48 hrs. The siRNA transfection efficiency was determined by RT-PCR and western blot (Supplementary Fig. 3a-c).

Cell contraction assay

RASMCs contraction was detected using a Cell Contraction Assay Kit (Cell Biolabs, Inc., San Diego, CA, USA, Cat#: CBA-201) according to the manufacturer's instructions[49]. RASMCs were treatment siRNA for 48 hrs with or without Ang II for 24 hrs, and then cultured in collagen gel for 48 hrs to develop mechanical load. The surface image of the collagen gel was captured via digital camera, and analyzed using Image-Pro Plus software (Media Cybernetics, USA). The percentage of contraction was the ratio of gel contracted surface area to the dish bottom.

Statistics and reproducibility

Statistical analysis was performed using GraphPad Prism 8 (GraphPad Software Inc., La Jolla, CA). Data are expressed as means ± standard error of mean (SEM). Two-tailed Student's t-test was performed to compare differences between two groups from at least three independent experiments. Two-way ANOVA with Bonferroni's post hoc test was performed to compare differences between multiple groups, using at least three independent experiments. P value < 0.05 was considered statistically significant.

Data availability

Raw data of genotyping and western blot are provided in Supplementary Data 1. Source data underlying the graphs are provided in Supplementary Data 2. Other relevant data are available from the corresponding author upon request.

Declarations

Acknowledgements

This work was financially supported by the Chinese Academy of Medical Sciences Innovation Fund for Medical Sciences (2016-I2M-1-006), the National Natural Science Foundation of China (91739107) and National Key Research and Development Program of China Grants (2019YFA0801804 and 2019YFA0801703).

Author contributions

TF.F. and Y.H. designed experiments and analysed data. TF.F., Y.H., WP.G., TH.F., WJ.G., and X.S. performed experiments and analysed data. TF.F. and Y.H. wrote the manuscript. R.G. and J.W. conceived research question and oversaw the entirety of research.

Competing interests

The authors declare no competing interests.

References

1 Williams, B. *et al.* 2018 ESC/ESH Guidelines for the management of arterial hypertension. *European heart journal* **39**, 3021-3104, doi:10.1093/eurheartj/ehy339 (2018).

2 Fuchs, F. D. & Whelton, P. K. High Blood Pressure and Cardiovascular Disease. *Hypertension (Dallas, Tex. : 1979)* **75**, 285-292, doi:10.1161/hypertensionaha.119.14240 (2020).

3 Grassi, G. & Ram, V. S. Evidence for a critical role of the sympathetic nervous system in hypertension. *Journal of the American Society of Hypertension : JASH* **10**, 457-466, doi:10.1016/j.jash.2016.02.015 (2016).

4 Te Riet, L., van Esch, J. H., Roks, A. J., van den Meiracker, A. H. & Danser, A. H. Hypertension: renin-angiotensin-aldosterone system alterations. *Circulation research* **116**, 960-975, doi:10.1161/circresaha.116.303587 (2015).

5 Guzik, T. J. & Touyz, R. M. Oxidative Stress, Inflammation, and Vascular Aging in Hypertension. *Hypertension (Dallas, Tex. : 1979)* **70**, 660-667, doi:10.1161/hypertensionaha.117.07802 (2017).

6 Konukoglu, D. & Uzun, H. Endothelial Dysfunction and Hypertension. *Advances in experimental medicine and biology* **956**, 511-540, doi:10.1007/5584_2016_90 (2017).

7 Brown, I. A. M. *et al.* Vascular Smooth Muscle Remodeling in Conductive and Resistance Arteries in Hypertension. *Arterioscler Thromb Vasc Biol* **38**, 1969-1985, doi:10.1161/atvbaha.118.311229 (2018).

8 Mahfoud, F. *et al.* Treatment strategies for resistant arterial hypertension. *Deutsches Arzteblatt international* **108**, 725-731, doi:10.3238/arztebl.2011.0725 (2011).

9 Beavo, J. A. Cyclic nucleotide phosphodiesterases: functional implications of multiple isoforms. *Physiol Rev* **75**, 725-748, doi:10.1152/physrev.1995.75.4.725 (1995).

10 Bhat, A. *et al.* Phosphodiesterase-4 enzyme as a therapeutic target in neurological disorders. *Pharmacological research* **160**, 105078, doi:10.1016/j.phrs.2020.105078 (2020).

11 Lehrke, M. *et al.* PDE4 inhibition reduces neointima formation and inhibits VCAM-1 expression and histone methylation in an Epac-dependent manner. *J Mol Cell Cardiol* **81**, 23-33, doi:10.1016/j.yjmcc.2015.01.015 (2015).

12 De Franceschi, L. *et al.* Protective effects of phosphodiesterase-4 (PDE-4) inhibition in the early phase of pulmonary arterial hypertension in transgenic sickle cell mice. *FASEB journal : official publication of the Federation of American Societies for Experimental Biology* **22**, 1849-1860, doi:10.1096/fj.07-098921 (2008).

13 Delaunay, M., Osman, H., Kaiser, S. & Diviani, D. The Role of Cyclic AMP Signaling in Cardiac Fibrosis. *Cells* **9**, doi:10.3390/cells9010069 (2019).

14 Qin, X. *et al.* Smooth muscle-specific Gsα deletion exaggerates angiotensin II-induced abdominal aortic aneurysm formation in mice in vivo. *Journal of molecular and cellular cardiology* **132**, 49-59, doi:10.1016/j.yjmcc.2019.05.002 (2019).

15 Fantidis, P. The role of intracellular 3'5'-cyclic adenosine monophosphate (cAMP) in atherosclerosis. *Current vascular pharmacology* **8**, 464-472, doi:10.2174/157016110791330843 (2010).

16 Hara, Y. *et al.* Inhibition of MRP4 prevents and reverses pulmonary hypertension in mice. *J Clin Invest* **121**, 2888-2897, doi:10.1172/jci45023 (2011).

17 Kari, S., Vasko, V. V., Priya, S. & Kirschner, L. S. PKA Activates AMPK Through LKB1 Signaling in Follicular Thyroid Cancer. *Front Endocrinol (Lausanne)* **10**, 769, doi:10.3389/fendo.2019.00769 (2019).

18 Wang, S., Liang, B., Viollet, B. & Zou, M. H. Inhibition of the AMP-activated protein kinase-α2 accentuates agonist-induced vascular smooth muscle contraction and high blood pressure in mice. *Hypertension (Dallas, Tex. : 1979)* **57**, 1010-1017, doi:10.1161/hypertensionaha.110.168906 (2011).

19 Yin, L. M. *et al.* Transgelin-2 as a therapeutic target for asthmatic pulmonary resistance. *Sci Transl Med* **10**, doi:10.1126/scitranslmed.aam8604 (2018).

20 Li, H., Zuo, J. & Tang, W. Phosphodiesterase-4 Inhibitors for the Treatment of Inflammatory Diseases. *Front Pharmacol* **9**, 1048, doi:10.3389/fphar.2018.01048 (2018).

21 Li, H. *et al.* DC591017, a phosphodiesterase-4 (PDE4) inhibitor with robust anti-inflammation through regulating PKA-CREB signaling. *Biochemical pharmacology* **177**, 113958, doi:10.1016/j.bcp.2020.113958 (2020).

22 Houslay, M. D. & Adams, D. R. PDE4 cAMP phosphodiesterases: modular enzymes that orchestrate signalling cross-talk, desensitization and compartmentalization. *The Biochemical journal* **370**, 1-18, doi:10.1042/bj20021698 (2003).

23 Li, G. *et al.* Mechanisms underlying the anti-proliferative actions of adiponectin in human breast cancer cells, MCF7-dependency on the cAMP/protein kinase-A pathway. *Nutrition and cancer* **63**, 80-88, doi:10.1080/01635581.2010.516472 (2011).

24 Hutchinson, D. S., Chernogubova, E., Dallner, O. S., Cannon, B. & Bengtsson, T. Beta-adrenoceptors, but not alpha-adrenoceptors, stimulate AMP-activated protein kinase in brown adipocytes independently of uncoupling protein-1. *Diabetologia* **48**, 2386-2395, doi:10.1007/s00125-005-1936-7 (2005).

25 Medina, E. A. *et al.* PKA/AMPK signaling in relation to adiponectin's antiproliferative effect on multiple myeloma cells. *Leukemia* **28**, 2080-2089, doi:10.1038/leu.2014.112 (2014).

26 Shaw, R. J. *et al.* The tumor suppressor LKB1 kinase directly activates AMP-activated kinase and regulates apoptosis in response to energy stress. *Proc Natl Acad Sci U S A* **101**, 3329-3335, doi:10.1073/pnas.0308061100 (2004).

27 Huang, Y. *et al.* Resveratrol prevents sarcopenic obesity by reversing mitochondrial dysfunction and oxidative stress via the PKA/LKB1/AMPK pathway. *Aging* **11**, 2217-2240, doi:10.18632/aging.101910 (2019).

28 Brown, M. J. & Haydock, S. Pathoaetiology, epidemiology and diagnosis of hypertension. *Drugs* **59 Suppl 2**, 1-12; discussion 39-40, doi:10.2165/00003495-200059002-00001 (2000).

29 Abrams, W. B. Pathophysiology of hypertension in older patients. *The American journal of medicine* **85**, 7-13, doi:10.1016/0002-9343(88)90343-9 (1988).

30 Martin-Chouly, C. A. *et al.* Modulation of matrix metalloproteinase production from human lung fibroblasts by type 4 phosphodiesterase inhibitors. *Life sciences* **75**, 823-840, doi:10.1016/j.lfs.2004.01.021 (2004).

31 Dunkern, T. R., Feurstein, D., Rossi, G. A., Sabatini, F. & Hatzelmann, A. Inhibition of TGF-beta induced lung fibroblast to myofibroblast conversion by phosphodiesterase inhibiting drugs and activators of soluble guanylyl cyclase. *European journal of pharmacology* **572**, 12-22, doi:10.1016/j.ejphar.2007.06.036 (2007).

32 Kuwabara, J. T. & Tallquist, M. D. Tracking Adventitial Fibroblast Contribution to Disease: A Review of Current Methods to Identify Resident Fibroblasts. *Arterioscler Thromb Vasc Biol* **37**, 1598-1607, doi:10.1161/atvbaha.117.308199 (2017).

33 Dinh, Q. N., Drummond, G. R., Sobey, C. G. & Chrissobolis, S. Roles of inflammation, oxidative stress, and vascular dysfunction in hypertension. *BioMed research international* **2014**, 406960, doi:10.1155/2014/406960 (2014).

34 Savoia, C. & Schiffrin, E. L. Inflammation in hypertension. *Current opinion in nephrology and hypertension* **15**, 152-158, doi:10.1097/01.mnh.0000203189.57513.76 (2006).

35 Ren, J. & Crowley, S. D. Role of T-cell activation in salt-sensitive hypertension. *American journal of physiology. Heart and circulatory physiology* **316**, H1345-h1353, doi:10.1152/ajpheart.00096.2019 (2019).

36 Dingwell, L. S. *et al.* B-Cell Deficiency Lowers Blood Pressure in Mice. *Hypertension (Dallas, Tex. : 1979)* **73**, 561-570, doi:10.1161/hypertensionaha.118.11828 (2019).

37 Chan, C. T. *et al.* Obligatory Role for B Cells in the Development of Angiotensin II-Dependent Hypertension. *Hypertension (Dallas, Tex. : 1979)* **66**, 1023-1033, doi:10.1161/hypertensionaha.115.05779 (2015).

38 Drummond, G. R., Vinh, A., Guzik, T. J. & Sobey, C. G. Immune mechanisms of hypertension. *Nature reviews. Immunology* **19**, 517-532, doi:10.1038/s41577-019-0160-5 (2019).

39 Yun, S. *et al.* Interaction between integrin α5 and PDE4D regulates endothelial inflammatory signalling. *Nature cell biology* **18**, 1043-1053, doi:10.1038/ncb3405 (2016).

40 Ariga, M. *et al.* Nonredundant function of phosphodiesterases 4D and 4B in neutrophil recruitment to the site of inflammation. *Journal of immunology (Baltimore, Md. : 1950)* **173**, 7531-7538, doi:10.4049/jimmunol.173.12.7531 (2004).

41 Jin, S. L., Ding, S. L. & Lin, S. C. Phosphodiesterase 4 and its inhibitors in inflammatory diseases. *Chang Gung medical journal* **35**, 197-210, doi:10.4103/2319-4170.106152 (2012).

42 Ould Amer, Y. & Hebert-Chatelain, E. Mitochondrial cAMP-PKA signaling: What do we really know? *Biochimica et biophysica acta. Bioenergetics* **1859**, 868-877, doi:10.1016/j.bbabio.2018.04.005 (2018).

43 Jiang, S. *et al.* AMPK: Potential Therapeutic Target for Ischemic Stroke. *Theranostics* **8**, 4535-4551, doi:10.7150/thno.25674 (2018).

44 Daskalopoulos, E. P., Dufeys, C., Beauloye, C., Bertrand, L. & Horman, S. AMPK in Cardiovascular Diseases. *Experientia supplementum (2012)* **107**, 179-201, doi:10.1007/978-3-319-43589-3_8 (2016).

45 Dong, Y. *et al.* Reduction of AMP-activated protein kinase alpha2 increases endoplasmic reticulum stress and atherosclerosis in vivo. *Circulation* **121**, 792-803, doi:10.1161/circulationaha.109.900928 (2010).

46 Lob, H. E., Schultz, D., Marvar, P. J., Davisson, R. L. & Harrison, D. G. Role of the NADPH oxidases in the subfornical organ in angiotensin II-induced hypertension. *Hypertension (Dallas, Tex. : 1979)* **61**, 382-387, doi:10.1161/hypertensionaha.111.00546 (2013).

47 Daugherty, A., Rateri, D., Hong, L. & Balakrishnan, A. Measuring blood pressure in mice using volume pressure recording, a tail-cuff method. *Journal of visualized experiments : JoVE*, doi:10.3791/1291 (2009).

48 Wang, X. *et al.* Nuciferine relaxes rat mesenteric arteries through endothelium-dependent and -independent mechanisms. *British journal of pharmacology* **172**, 5609-5618, doi:10.1111/bph.13021 (2015).

49 Malhotra, R. *et al.* HDAC9 is implicated in atherosclerotic aortic calcification and affects vascular smooth muscle cell phenotype. *Nature genetics* **51**, 1580-1587, doi:10.1038/s41588-019-0514-8 (2019).

Figures

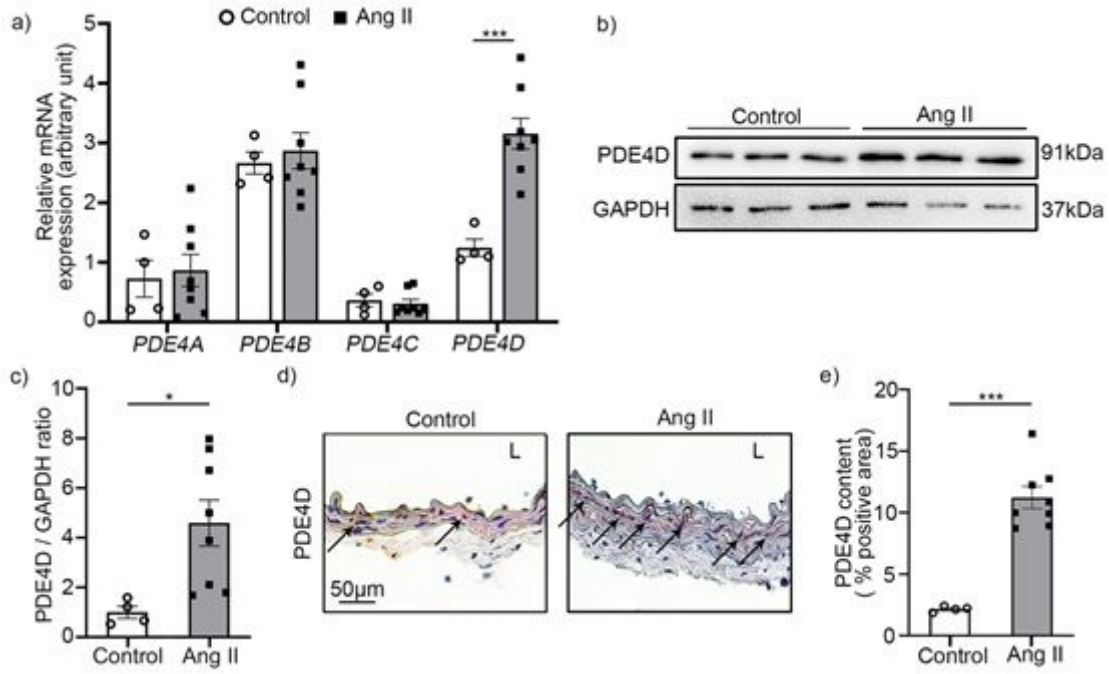

Figure 1

PDE4D expression is upregulated in hypertensive mice. a) Real-time polymerase chain reaction (RT-PCR) was used to measure mRNA expression of Pde4a, Pde4b, Pde4c, and Pde4d in the aorta tissues of control mice and hypertensive mice. b) Representative western blot showing PDE4D expression in aorta

tissues. c) Quantification of PDE4D expression normalized to glyceraldehyde-3-phosphate dehydrogenase (GAPDH) protein. d) Representative immunohistochemical staining of PDE4D. Arrows indicate positive areas. e) Quantification of the percentage of PDE4D-positive area. n = 4 in control group, n = 8 in hypertensive group. Data are expressed as mean ± SEM. *P < 0.05, ***P < 0.001. L: lumen.

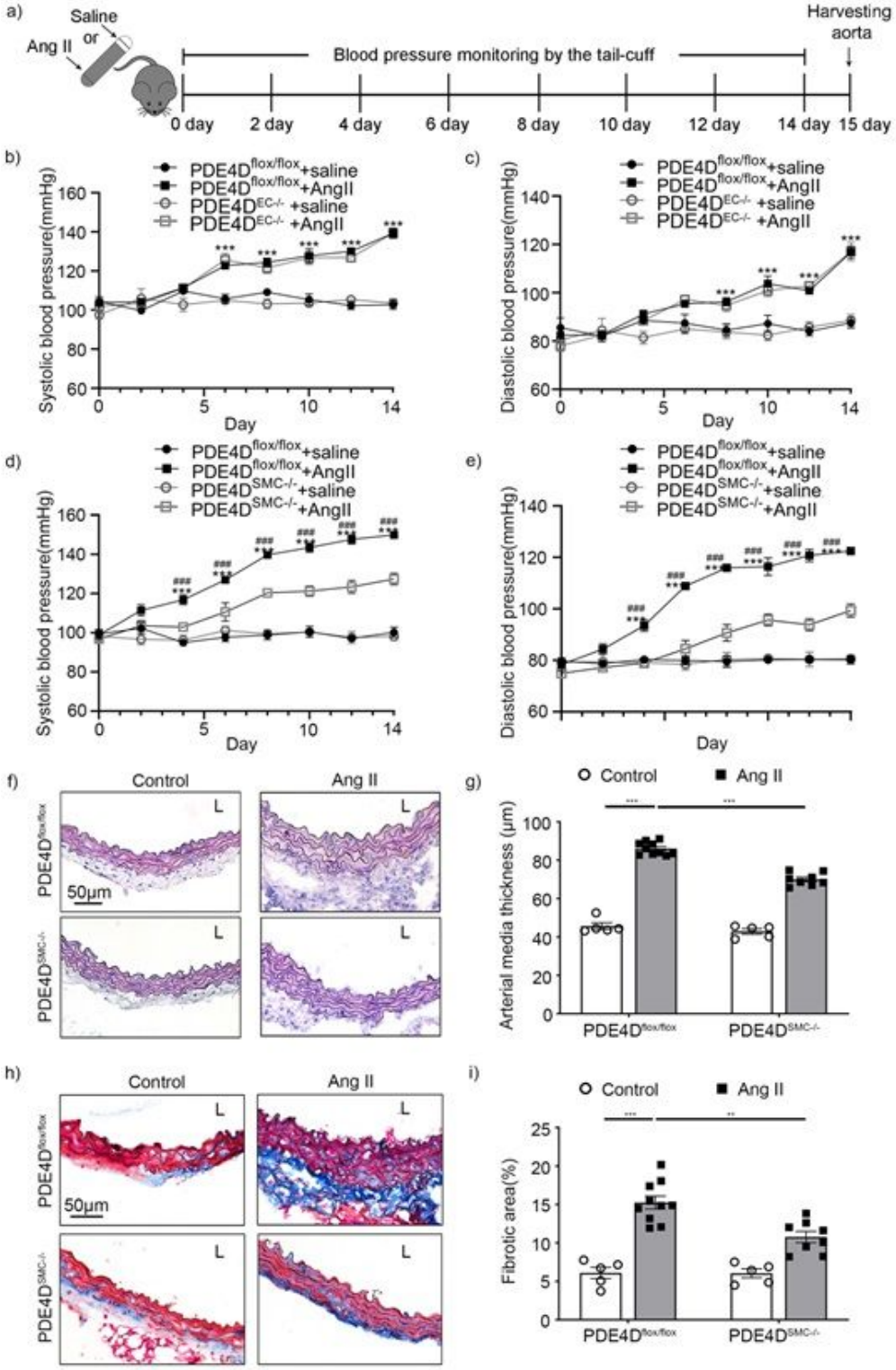

Figure 2

PDE4D in SMCs contributes to Ang II-induced mouse hypertension. a) Scheme of hypertensive mice inducement. b) SBP and c) DBP were measured in PDE4Dflox/flox and PDE4DEC-/- mice, with or without Ang II treatment: n = 5 in PDE4Dflox/flox + saline group, n = 8 in PDE4Dflox/flox + Ang II group, n = 5 in PDE4DEC-/- + saline group, and n = 8 in PDE4DSMC-/- + Ang II group. d) SBP and e) DBP were measured in PDE4Dflox/flox and PDE4DSMC-/- mice, with or without Ang II treatment: n = 5 in PDE4Dflox/flox + saline group, n = 10 in PDE4Dflox/flox + Ang II group, n = 5 in PDE4DSMC-/- + saline group, and n = 8 in PDE4DSMC-/- + Ang II group. ***P < 0.001 for PDE4Dflox/flox + Ang II group vs. PDE4Dflox/flox + saline group, and ###P < 0.001 for PDE4DSMC-/- + Ang II group vs. PDE4Dflox/flox + Ang II group. f) Representative H&E staining under the indicated experimental conditions. g) Measurement of arterial wall media thickness in f); n = 5 / per group randomly. h) Representative masson-trichrome staining under the indicated experimental conditions. i) Quantification of the positively stained area to the aortic wall area in h); n = 5 / per group randomly. Data are expressed as mean ± SEM. **P < 0.01, ***P < 0.001. L: lumen.

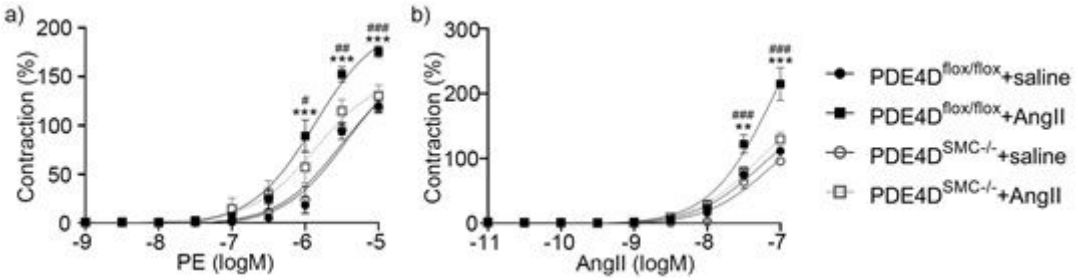

Figure 3

Pde4d deficiency in SMCs affects vasocontraction. Concentration-response curves for a) PE and b) Ang II induced vasocontraction of mesenteric resistance artery from PDE4Dflox/flox and PDE4DSMC-/- mice with or without Ang II treatment (n = 5 in PDE4Dflox/flox + saline group, n = 10 in PDE4Dflox/flox + Ang II group, n = 5 in PDE4DSMC-/- + saline group, and n = 8 in PDE4DSMC-/- + Ang II group). Data are expressed as mean ± SEM. **P < 0.01 and ***P < 0.001 for PDE4Dflox/flox + Ang II group vs. PDE4Dflox/flox + saline group. #P < 0.05, ##P < 0.01, and ###P < 0.001 for PDE4DSMC-/- + Ang II group vs. PDE4Dflox/flox + Ang II group.

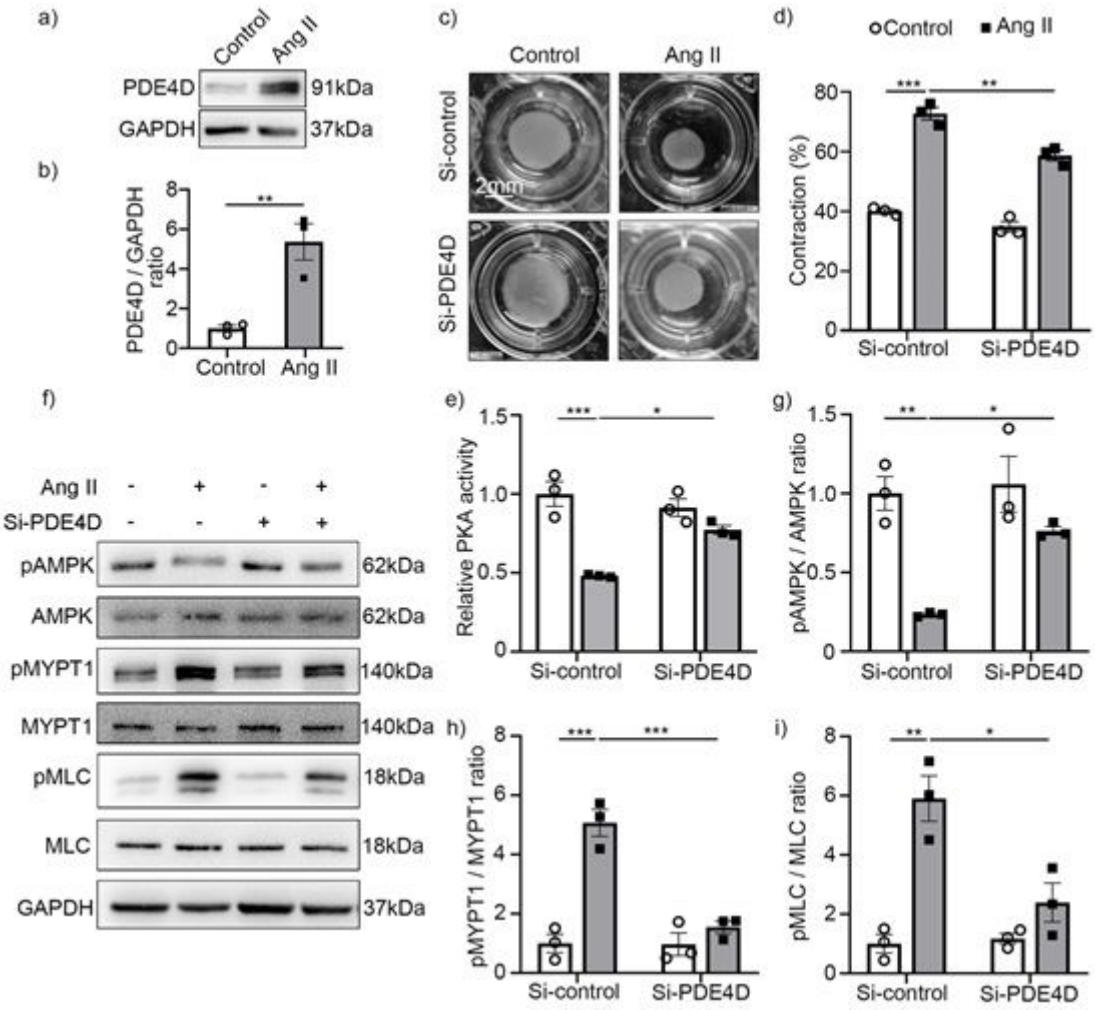

Figure 4

PDE4D promotes SMC contraction through the PKA-AMPK-MYPT1-MLC signaling pathway in vitro. a) Representative western blot showing PDE4D expression in control and Ang II-stimulated RASMCs. b) Quantification of PDE4D expression normalized to GAPDH protein. c) Representative images showing RASMCs contraction. d) Quantification of RASMCs contraction. e) Protein kinase A (PKA) kinase activity in RASMCs. f) Representative western blot exhibiting phosphor-AMPK (pAMPK), AMPK, phospho-MYPT1 (pMYPT1), MYPT1, phospho-MLC (pMLC), and MLC expression in RASMCs. g) Quantification of pAMPK expression normalized to AMPK protein. h) Quantification of pMYPT1 expression normalized to MYPT1 protein. i) Quantification of pMLC expression normalized to MLC protein. Data are expressed as mean ± SEM; n = 3 per group. *P < 0.05, **P < 0.01, and ***P < 0.001.

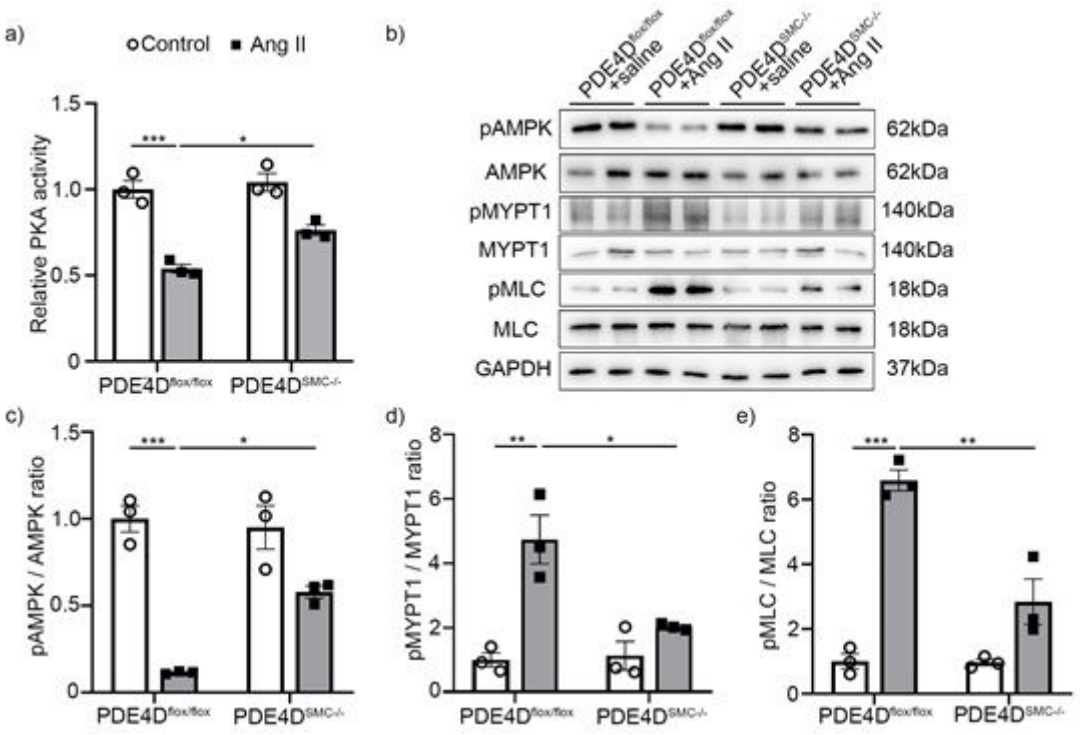

Figure 5

PDE4D promotes vasocontraction through the PKA-AMPK-MYPT1-MLC signaling pathway in vivo. a) PKA kinase activity in aorta tissues . b) Representative western blot showing pAMPK, AMPK, pMYPT1, MYPT1, pMLC, and MLC expression in aorta tissues from PDE4Dflox/flox and PDE4DSMC-/- mice with or without Ang II treatment. c) Quantification of pAMPK expression normalized to AMPK protein. d) Quantification of pMYPT1 expression normalized to MYPT1 protein. e) Quantification of pMLC expression normalized to MLC protein. Data are expressed as mean ± SEM; n = 3 per group. *P < 0.05, **P < 0.01, and ***P < 0.001.

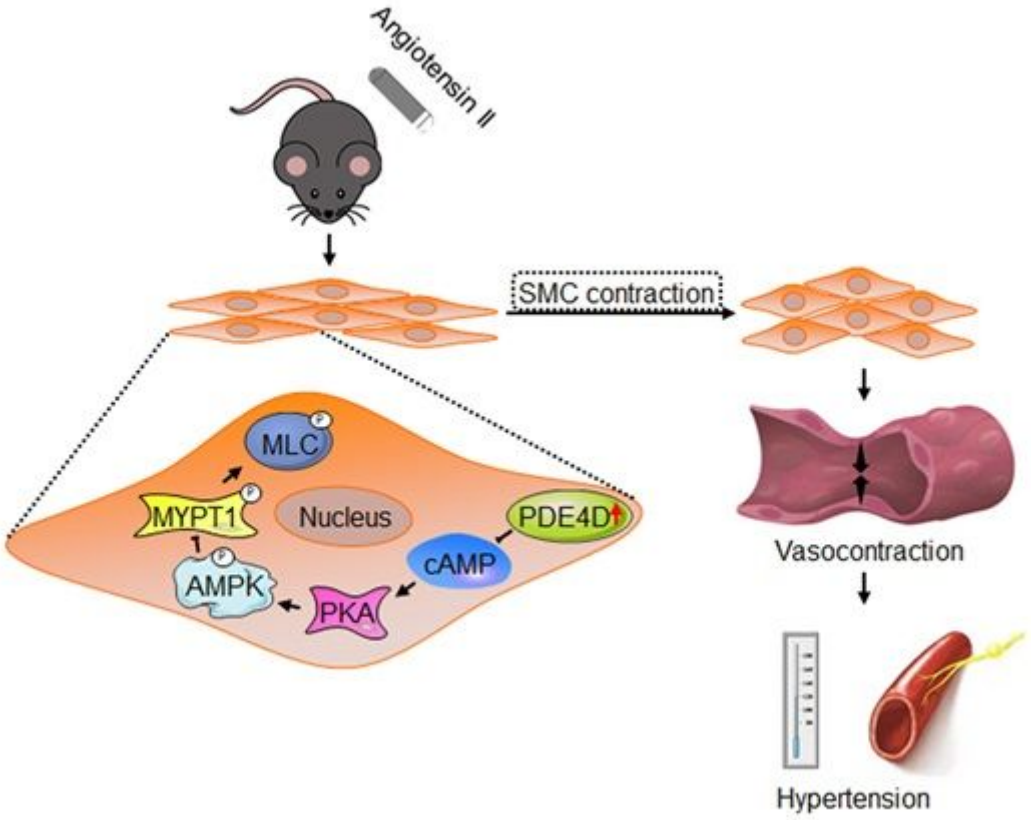

Figure 6

PDE4D promotes Ang II-induced hypertension in mice. PDE4D exacerbates Ang II-induced vasocontraction by affecting SMC contraction, consequently contributing to hypertension. The mechanism by which PDE4D aggravates SMC contraction likely involves the PKA-AMPK-MYPT1-MLC signaling pathway.

Supplementary Files

This is a list of supplementary files associated with this preprint. Click to download.

- SupplementaryData1.docx
- SupplementaryData2.xlsx
- SupplementaryFigureandTable.docx